Evaluation of onboard stability assessment techniques under real operational conditions

Lucía Santiago Caamaño [a],[*], Marcos Míguez González [a], Sandra Allegue García [b], Vicente Díaz Casás [a]

[a] *Grupo Integrado de Ingeniería, Campus Industrial de Ferrol, Universidade da Coruña, Ferrol, Spain*
[b] *Navantia S.A., Ferrol, Spain*

ABSTRACT

Stability-related accidents and crew lack of training are among the main causes of fatalities in the fishing fleet. Onboard stability guidance systems have been proposed by many authors as a possible solution. These guidance systems have been evolving from colour-coded posters to computer-based systems. However, their real-time operation without crew interaction is not solved yet.

This work presents the validation of a methodology proposed by the authors in previous works for estimating the natural roll frequency of the vessel in real-time and thus the metacentric height. The performance of this method, based on the analysis of the roll motion, is tested during a fishing campaign of a mid-sized trawler, showing very promising results.

1. Introduction

As it is well known, fishing is one of the most dangerous occupations worldwide. Stability failures in combination with crew lack of training in this matter and the absence of objective stability information on board are among the main causes of accidents involving fatalities. In particular, small and mid-sized fishing vessels are the most affected by this situation (Gudmundsson, 2013; Jensen et al., 2014; Míguez González et al., 2012).

Onboard stability guidance systems together with training programs have been proposed by several authors as a way to try to reduce the number of fatalities (Míguez González et al., 2012). Their main objective is to provide the skipper with simplified and easy to understand stability information and, if possible (and especially important in small and medium-sized vessels) using a system with a reduced cost of acquisition, installation and maintenance.

The first proposals on this matter were based on diagrams of the vessel representing different loading conditions or operational situations, associated with a colour code representing the inherent risk of each of those combinations. Some examples are the Womack Matrix, the Wolfson Stability Guidance and the recommendations of the Norwegian Maritime Directorate (Scarponi, 2017; Viggosson, 2009; Wolfson Unit,

2004; Womack, 2003). Although the performance of these first attempts was satisfactory, they presented two major drawbacks. On one hand, they relied on the subjective appreciation of the crew. And on the other hand, their use became more and more complex as the size of the vessel (and so of the diagram) increased.

Regarding the most modern approaches to stability guidance, they have the objective of minimizing the need for crew interaction and subjectivity of the stability evaluation. In order to do so, many of them are based on the estimation of the natural roll frequency of the vessel from the analysis of roll motion, following the premise that this parameter is largely related to the vessel metacentric height (one of the key parameters affecting transverse stability).

In this line, the first proposals date back to the works of Koyama in 1982, which consisted of estimating the natural roll period of the vessel using a pendulum and a computer that estimated the RMS of its motion, triggering an alarm if necessary (Koyama, 1982). More recently, Terada et al. developed two methodologies for the estimation of the vessel's natural roll frequency in real-time and, from it, the vessel stability. The first one (Terada et al., 2018b), was based on the application of an autoregressive procedure and general state-space modelling applied to the roll motion of the vessel, while in the second one (Terada et al., 2018a) the Markov chain Monte Carlo (MCMC) method is applied with

the same objective. In both cases, the authors indicate that further validation is needed to verify the obtained results.

On the basis of this same principle (real-time estimation of the natural roll frequency to derive the stability parameters of the vessel), the authors of this work have developed their own proposal. It consists of a methodology based on the use of the Fast Fourier Transform (*FFT*) for estimating in real-time the natural roll frequency of the vessel and thus, the metacentric height. Firstly, in (Míguez González et al., 2016; Santiago Caamaño et al., 2018), an initial approach to this system was presented, and the influence of the different involved parameters in the estimation of the vessel's stability from the natural roll frequency was analysed. And secondly, in (Míguez González et al., 2017), an evolution of the previous methodology, based on the recursive application of the *FFT* and fitted for its use in real-time applications, was presented.

The main advantage of this methodology is that crew interaction with the system is not necessary, so the resulting stability estimations are done in a much more objective way. The performance of this methodology was tested with simulated roll motion time series from a one degree of freedom nonlinear roll mathematical model (Míguez González et al., 2017) and also from experimental towing tank tests (Santiago Caamaño et al., 2018). In this work, and with the objective of complementing the previous results, the performance of this last methodology is evaluated in a fully realistic environment, using roll motion data obtained from a 19-h fishing campaign of a mid-sized stern trawler.

2. Real-Time natural roll frequency estimation methodology

The proposed methodology is based on the one presented in (Míguez González et al., 2017) and includes some modifications to increase its performance.

It is based on the assumption that the peak frequency of the roll spectrum, estimated by using the Fast Fourier Transform, corresponds to the natural roll frequency. Nevertheless, the approach of the method is oriented to deal with the limitations induced by the *FFT*: the frequency resolution, the variation of the roll spectrum in time due to changes in the vessel's loading condition and the need to use overlapped analysis in real-time.

The computation of the roll power spectrum, which is used for the natural roll frequency estimation, is done considering the following procedure. Firstly, a series of roll spectra are computed according to Equation (1) recursively for a group of overlapped roll time series, which have a length denominated "Analysis Time", and which are sampled at a "Sample Time" rate.

$$S(\omega) = \frac{|FFT(x(t))|^2}{N} \tag{1}$$

Where $x(t)$ represents the roll motion time series and N the length of the signal.

Considering the fact that the frequency resolution of the *FFT* directly depends on the length of the time series to which it is applied, a longer "Analysis Time" will lead to a more discretized spectrum, but at the same time, a too long "Analysis Time" may hide possible changes in stability. During a predefined "Averaging Time", these roll power spectra are computed and then averaged, obtaining the so-called "Averaged

Spectrum". This spectrum represents the average situation of the vessel during this "Averaging Time". Although it has the same frequency resolution as the single chunk spectra, this approach reduces the possibility that spectra largely influenced by waves or other causes may lead to wrong stability estimations. Considering that the "Analysis Time" should be kept as short as possible, the obtained spectra are, in most cases, lacking frequency resolution, presenting a multi-peaked scarce shape and reducing the precision of the identification of the maximum value (which theoretically corresponds to the natural roll frequency). The outline of this procedure is described in Fig. 1.

In order to increase the smoothness and frequency resolution of the averaged spectra, and to improve the peak identification, the following procedure is applied. Firstly, a 5 point moving average technique is used to smooth the spectra. This function recalculates each point of the spectrum $S(\omega_i)$ by using the following expression:

$$S_{smooth}(\omega_i) = \frac{1}{5} \sum_{j=i-2}^{i+2} S(\omega_j) \tag{2}$$

And secondly, and with the objective of increasing the frequency resolution and improving the detection of the peak corresponding to the natural roll frequency of the vessel, a simple parametric model based on the superposition of 3 Gaussian functions is fitted to each spectrum. Each Gaussian has three parameters, and the number of functions has been defined to allow the fitting of three overlapping spectra, corresponding to wave and wind excitations and ship roll motion. The process for fitting this model to the spectrum consists of two steps: the first step approximates the adjustment parameters through a minimization process based on a genetic algorithm; and the second one uses a nonlinear least-squares fitting to determine the final parameters of the model (Míguez González et al., 2017). This Averaged Spectrum, after the aforementioned smoothing and fitting procedures, is the one used for estimating the natural roll frequency of the vessel (which is supposed to coincide with that corresponding to the maximum of the spectrum).

Furthermore, and in order to limit the natural roll frequency search space, and to improve the performance of the methodology, an expected maximum and minimum value of the roll natural frequency have been used. In case the obtained roll natural frequency estimate would be higher or lower than those values, its value is replaced by the corresponding limit. Even though during sailing the loading condition of the vessel may change in a sensible way, the resulting *GM* and so the roll natural frequency should be within more constrained limits than $0 \leq \omega_0 \leq \infty$. For this reason, the range of variation has been limited between the interval $\omega_{0,min} \leq \omega_0 \leq \omega_{0,max}$, being $\omega_{0,max}$ the expected maximum and $\omega_{0,min}$ the minimum expected value.

The expected maximum for a given vessel is the one corresponding to the loading condition of the stability booklet with the highest *GM*, plus a 15% margin. Regarding the minimum expected roll natural frequency, it is associated with the minimum stability level necessary to keep the vessel heel angle under 15° under a 30-knot lateral wind (computing heeling moments following IMO WeC procedures (IMO, 2008)). These limits provide a conservative view of the whole range of possible natural roll frequencies.

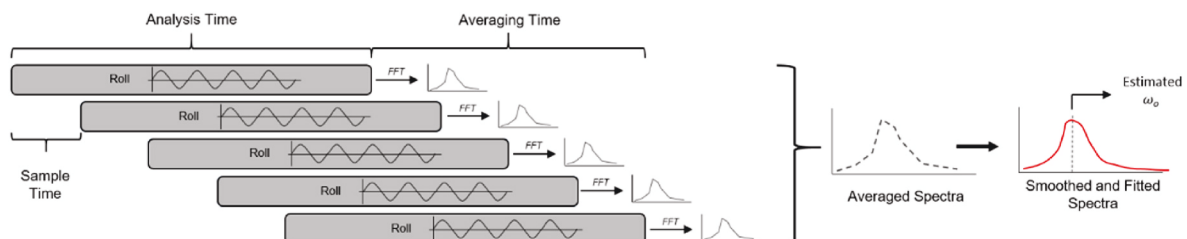Finally, and in order to remove the outliers of the natural roll

Fig. 1. Outline of the roll motion spectra computation procedure.

estimations, a Hampel filter has been applied to the obtained results (Pearson et al., 2016). This filter computes, on the one hand, the median for each sample and its six surrounding samples, three per side, and on the other hand, its standard deviation. If a sample differs from the median by more than three standard deviations, it is substituted by the median.

In this work, the performance of the described methodology, of the one with the aforementioned constraints of the natural roll frequency estimations and of the one with these constraints and the Hampel filter, are analysed using roll motion data from a full-scale test campaign of a medium-sized stern trawler. In order to evaluate this performance of the estimation, the median and the 5% and 95% percentiles are used as statistical measures to find the most probable values of the estimated natural roll frequency above and below the target value. Moreover, the deviation from the target value has been calculated following Equation (3), so that it can be easily checked whether or not most of the estimations are close to the target value.

$$Dev. [\%] = \frac{(\widehat{\omega} - \omega)}{\omega} \times 100 \quad (3)$$

Being $\widehat{\omega}$ the estimated natural roll frequency using the described methodology and ω the target value.

3. Full-scale fishing campaign

As it has been already described, in previous works the authors have analysed the performance of the proposed methodology by using roll motion data from both a nonlinear mathematical roll model as well as from towing tank tests. However, in this work and with the objective of testing the behaviour of the system in a more realistic environment, real data from a mid-sized pair stern trawler during operation, have been used. These data have been obtained during a 19-h fishing campaign, on board a ship that is a representative of the coastal trawling Spanish fleet.

This test vessel is based in A Coruña port and fishes in Galician waters (Northwest Spain) with her sistership, in a fishing ground close to the Vilano-Sisargas SeaWatch buoy. Fig. 2 shows on the left the fishing area (highlighted with the red dashed line) and the buoy position (the red circle) and on the right the track path followed by the ship during the fishing campaign under analysis in this work. The track path was obtained from the GPS.

During this campaign, vessel motions, loading condition, heading, speed and environmental conditions have been monitored. Vessel motions have been measured by using an Xsense IMU, while speed, heading and route/location were obtained by using GPS. Regarding wave and wind conditions, hourly data from the Villano-Sisargas buoy have been provided by Puertos del Estado (Puertos del Estado, 2020). They include significant wave height, peak period and mean wave direction, and also

mean wind speed and direction. In order to monitor the vessel's loading condition, all weight items changing during the operation, such as consumptions, nets, fish catch, etc., together with drafts, were manually monitored by one of the authors, who was on board the vessel during the campaign.

3.1. Test vessel

The test vessel is a pair stern trawler, typical of the Galician fishing fleet. Her main characteristics are presented in Table 1. Fig. 3 shows a picture of the vessel and her hull forms. This test vessel has very similar main dimensions, hull forms and arrangement to the one used in previous works by some of the authors (Míguez González et al., 2017; Míguez González and Bulian, 2018; Santiago Caamaño et al., 2019), where a mathematical model and towing tank tests were done. This similarity makes it possible to directly compare results from these other works to those obtained with this real vessel.

3.2. Target natural roll frequency

In order to have a comparative value to check the performance of the natural roll frequency estimation methodology, the loading condition of the vessel during the whole campaign has been manually monitored, including tank filling levels, approximate fish weight and location, situation and weight of fishing nets and other equipment and number of people on board. Ship lightweight has been obtained from the vessel compulsory inclining experiment, included in the stability booklet.

In consequence, the metacentric height during sea trials has been estimated, including the free surface effect, as:

$$GM = KB + BM - KG - FSE \quad (4)$$

Being KB the vertical centre of buoyancy, BM the transversal metacentric radius, KG the vertical centre of gravity and FSE the free surface effect.

The natural roll frequency has been calculated using the Weiss formula to approximate the ship's inertia:

Table 1
Test vessel: main characteristics.

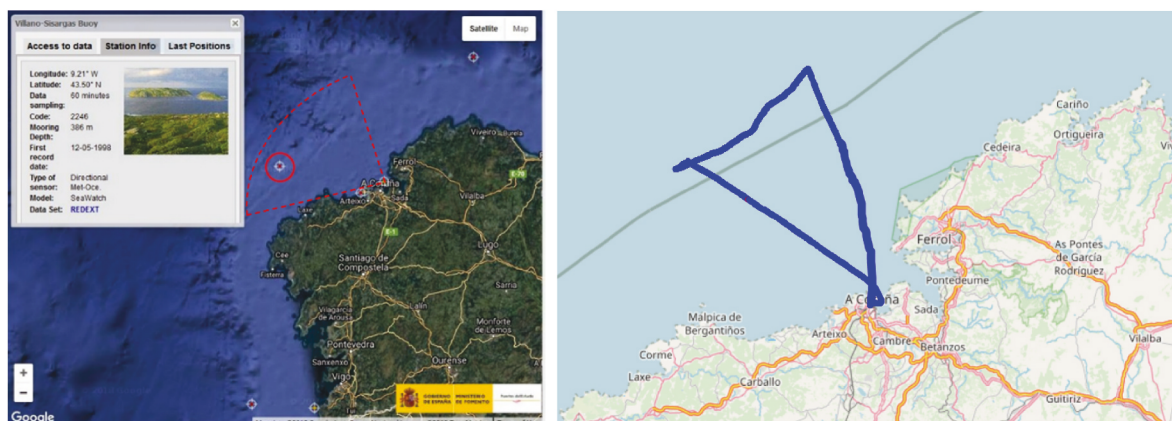|	
Overall Length	30.70 m
Length Between Perpendiculars	25.20 m
Beam	8.00 m
Depth	3.60 m
Design Draft	3.55 m
Displacement	504 t

Fig. 2. Left: Fishing area and Vilano-Sisargas SeaWatch buoy position (Míguez González et al., 2018; Puertos del Estado, 2020). Right: Track path followed by the ship during the fishing campaign under analysis.
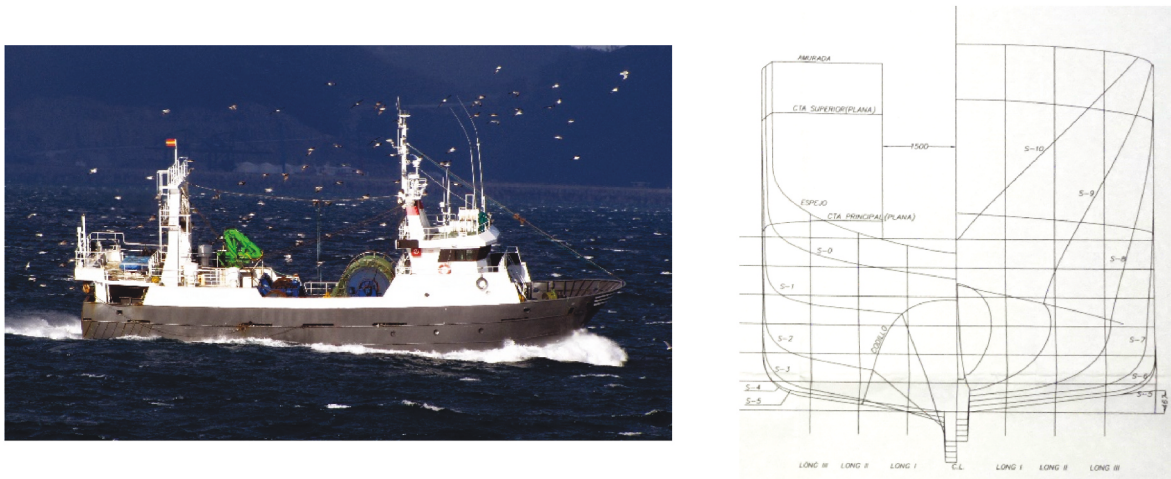
Fig. 3. Left: Test vessel. Photo courtesy of José R. Montero. Right: Test vessel hull sections.

$$\omega_0 = \sqrt{\frac{g \cdot GM}{k_{xx}^2}} \qquad (5)$$

Being k_{xx} the roll gyradius, taken as $k_{xx} = 0.4 \cdot B$ (Santiago Caamaño et al., 2018).

During the campaign 5 loading conditions have been distinguished:

1. **Departure from the port, 82.3% of fuel oil.** The vessel leaves the port with her sistership and navigates towards the fishing ground.
2. **Arrival at the fishing ground.** The vessel arrives at the fishing ground and starts the fishing operation.
3. **End of fishing, 7.61% of catches, catches on deck.** The fishing operation is finished and the net is discharged on deck containing 7.500 tons of fish. The maximum hold capacity of the vessel is 98.544 t. Thus, the percentage of total catches in this campaign is 7.61%.
4. **End of fishing, 7.61% of catches, catches in hold.** The catches are moved to the hold while the vessel starts navigating towards the port.
5. **Arrival at the port**.

Table 2 shows the summary of results obtained for the different loading conditions. It has to be mentioned that the trim has been calculated referring to the aft and forward perpendiculars.

3.3. Trial conditions

The whole fishing campaign lasted for a total of 19 h, including 3 h of sailing to the fishing ground, 10 h of fishing and 6 h of sailing back to port (the complete route is shown in Fig. 2).

In order to simplify the analysis and due to the limitations of the IMU, the total time of the fishing campaign has been divided into several time series.

Time series from 1 to 4 correspond to the loading condition "Departure from the port, 82.3% of fuel oil"; time series from 5 to 13 correspond to "Arriat val the fishing ground" and it is the period of time while the vessel is fishing (time series 5 coincides with the launch of the

net); time series 14 correspond to "End of fishing, 7.61% of catches, catches on deck"; time series 15 correspond to "End of fishing, 7.61% of catches, catches in hold" and time series 16 correspond to "Arrival to port". It has to be mentioned that, time series 2, 4, 6, 7 and 10 have been discarded from the analysis because they are too short or some erroneous measurements have been detected.

Table 3 shows the time series to analyse including vessel's speed and heading, corresponding metacentric height, target natural roll frequency, significant wave height (H_s), peak wave period (T_p) and absolute wave direction.

4. Results

In this section, the results of applying the presented methodology are shown. In this case, and following the same approach as done in (Míguez González et al., 2017), the "Analysis Time" has been taken as 180 s, the "Sample Time" as 10 s and the averaging of the spectra has been done for 120 s ("Averaging Time").

In order to illustrate how the constraints of the roll natural frequency in the methodology and the Hampel function work, the complete analysis of two time series is described in detail.

Fig. 4 shows the roll motion time series of Series 3, Fig. 5 displays the results of applying the methodology to the same time series, Fig. 6 shows the results after the limitation of the natural roll frequency and Fig. 8 the results after applying the Hampel filter as well. Table 4 presents the values of the median and the 5% and 95% percentiles (P5 and P95) corresponding to the three cases described before (methodology, methodology with constraints and methodology with constraints and Hampel filter).

As it can be seen in Fig. 5 and Table 4, the results of the methodology illustrate that the value of the estimated natural roll frequency median is very far from the target value ($\omega_0 = 0.691$ rad/s), not being satisfactory. However, in Fig. 6, it can be appreciated that after constraining the natural roll frequency output, the performance of the methodology is largely increased, being the obtained values of the roll natural frequency now much closer to the target value. Finally, in this case, the application

Table 2
Summary of results obtained for the different loading conditions.

	Trim (m)	Δ (t)	KG (m)	KB (m)	BM (m)	GM (m)	FSE (m)	Corrected GM (m)	ω_0 (rad/s)
Departure from the port, 82.3% of fuel oil	0.527	492.245	3.363	1.962	1.922	0.520	0.023	0.498	0.690
Arrival at the fishing ground	0.542	491.720	3.364	1.960	1.923	0.519	0.023	0.496	0.689
End of fishing, 7.61% of catches, catches on deck	0.675	498.248	3.403	1.980	1.906	0.483	0.022	0.460	0.664
End of fishing, 7.61% of catches, catches in hold	0.559	498.248	3.349	1.980	1.906	0.537	0.022	0.514	0.702
Arrival to port	0.574	497.723	3.350	1.978	1.908	0.536	0.023	0.513	0.701

Table 3
Trial conditions and summary of time series.

| Time series	Vessel speed (m/s)	Heading (deg)	Loading condition	Waves			GM (m)	ω_0 (rad/s)
				H_s (m)	T_p (s)	Direction (deg)		
1	4.78	342	Departure from the port, 82.3% of fuel oil	1.05	7.36	117	0.498	0.691
3	4.76	335	Departure frthe om port, 82.3% of fuel oil	1.05	6.06	23	0.498	0.691
5	1.09	224	Arrival at the fishing ground	0.94	7.81	147	0.496	0.689
8	1.05	212	Arrival at the fishing ground	0.94	10.8	275	0.496	0.689
9	1.06	240	Arrival at the fishing ground	0.88	10.6	280	0.496	0.689
11	0.96	248	Arrival at the fishing ground	0.91	10.3	272	0.496	0.689
12	0.87	248	Arrival the at fishing ground	0.94	10.4	26	0.496	0.689
13	0.76	74	Arrival the at fishing ground	0.86	10.2	271	0.496	0.689
14	3.11	124	End of fishing, 7.61% of catches, catches on deck	0.86	10.5	273	0.460	0.664
15	4.99	125	End of fishing, 7.61% of catches, catches in hold	0.82	10.6	270	0.514	0.702
16	4.77	124	Arrival to port	0.90	10.4	278	0.513	0.701
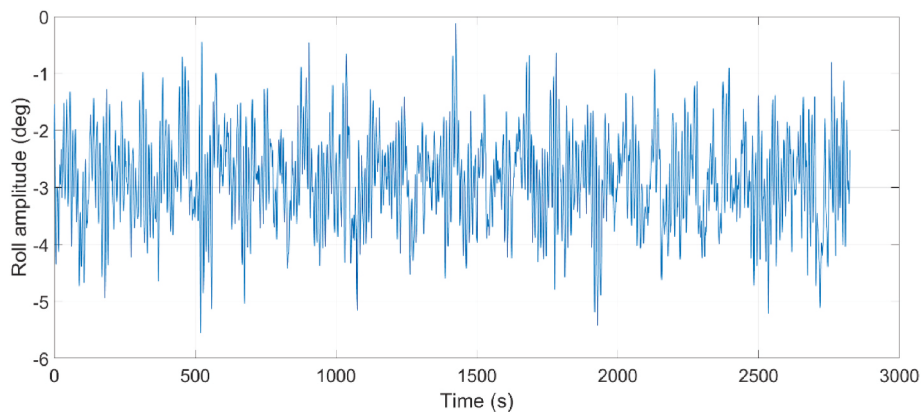
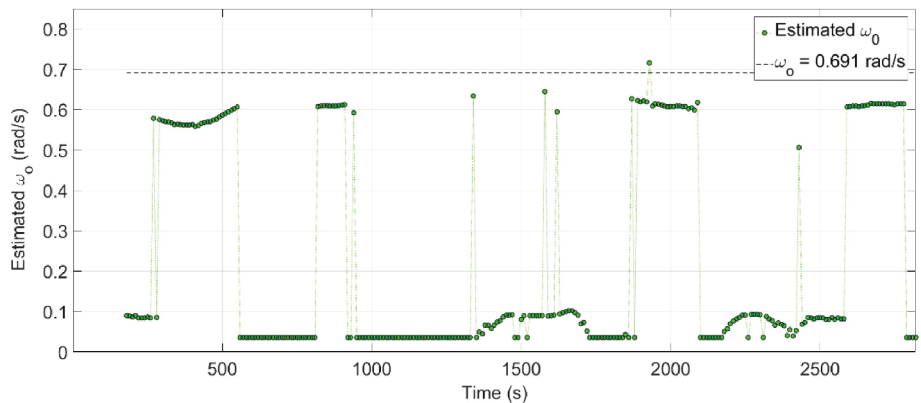
Fig. 4. Roll motion – Series 3.

Fig. 5. Roll natural frequency estimation – Series 3.

of the Hampel filter (Fig. 7) does not imply a noticeable change in the obtained results. Only the value of the 5% percentile slightly improves.

The second example is the one corresponding to the analysis of Series 5. Fig. 8 shows the roll motion time series, Fig. 9 the results of applying the methodology to the same time series, Fig. 10 the results after the limitation of the estimated natural roll frequency and Fig. 11 the results after also applying the Hampel filter. Table 5 presents again the values of the median and the 5% and 95% percentiles corresponding to the three cases described before (methodology, methodology with constraints and methodology with constraints and Hampel filter).

In this situation, the performance of the methodology (Fig. 9) is much better, being now the roll natural frequency estimations very close to the target value. However, there are some outliers that appear in frequencies close to 0 rad/s. Applying the constraints to the roll natural

frequency estimations (Fig. 10), decreases the number of outliers and improves the values of the median and the percentiles of the natural roll frequency estimates. Nevertheless, only with the use of the Hampel function the outliers completely disappear (Fig. 11).

Table 6 contains the summary of the results after applying the methodology, methodology with constraints and methodology with constraints and Hampel filter to all time series. They include the median, the 5% and 95% percentiles and the deviation from the median of the natural roll frequency estimates to the natural roll frequency target value.

Finally, Table 7 shows the obtained values of the GM from the resulting ω_0 and their deviation from the target GM of the loading condition.
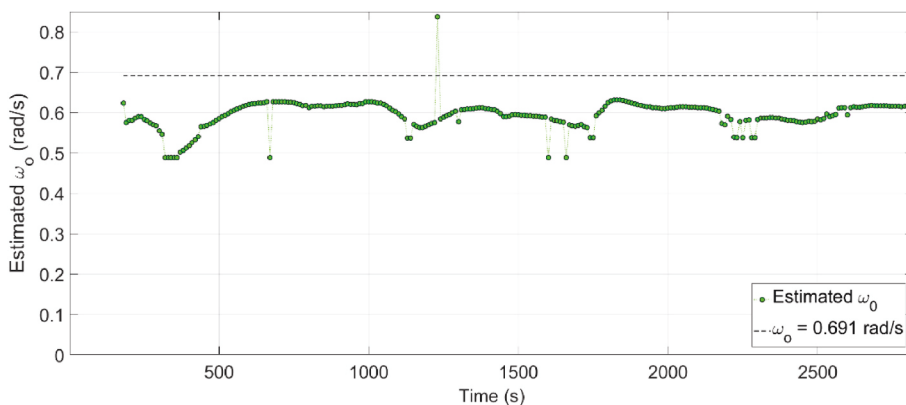
Fig. 6. Roll natural frequency estimation with constraints – Series 3.

Table 4
Summary of results – Series 3.

	Methodology	Methodology with constrains	Methodology with constraints and Hampel filter
Median (rad/s)	0.082	0.602	0.603
P5 (rad/s)	0.035	0.526	0.539
P95 (rad/s)	0.617	0.627	0.627

5. Discussion

From the results shown in Table 6, it can be concluded that, in general, the performance of the proposed methodology, the methodology with constraints and the methodology with constraints and Hampel filter is satisfactory.

Nevertheless, it can be appreciated that the original methodology presents the poorest estimations. For time series 1 and 2, the obtained results are very bad and for the rest, the deviations are the largest.

Adding the constraints to the roll natural frequency improves the results considerably, being the largest deviation −22.22%. However, the best results are obtained after applying the Hampel filter because completely removes the outliers in the estimates. In the majority of the
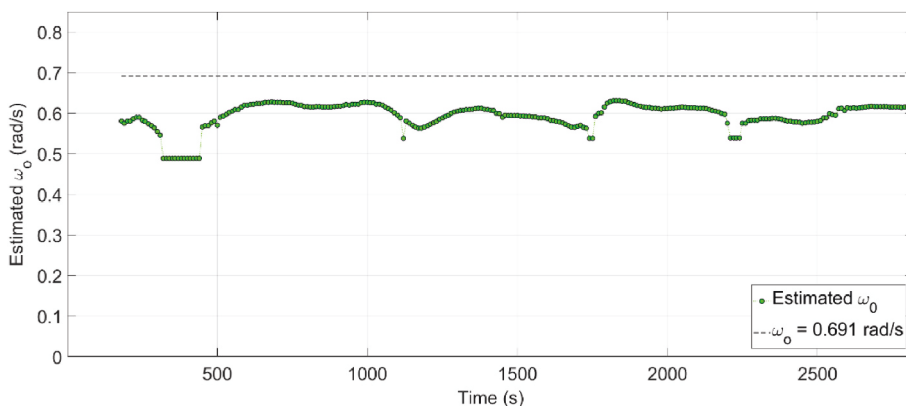

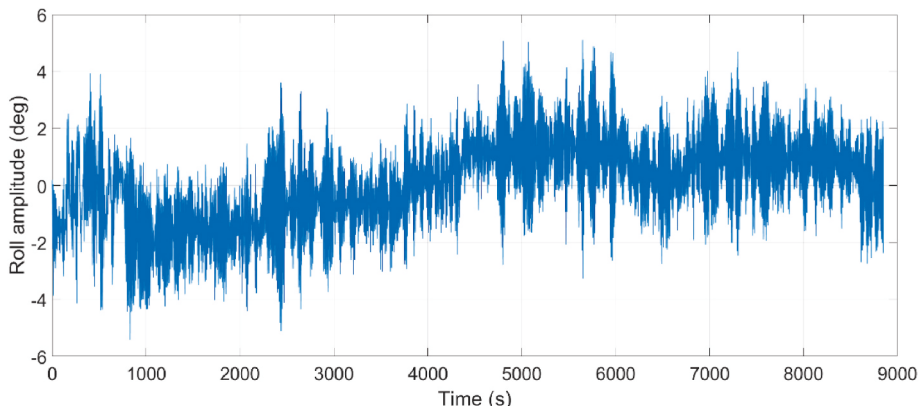**Fig. 7.** Roll natural frequency estimation with constraints and Hampel filter –Series 3.

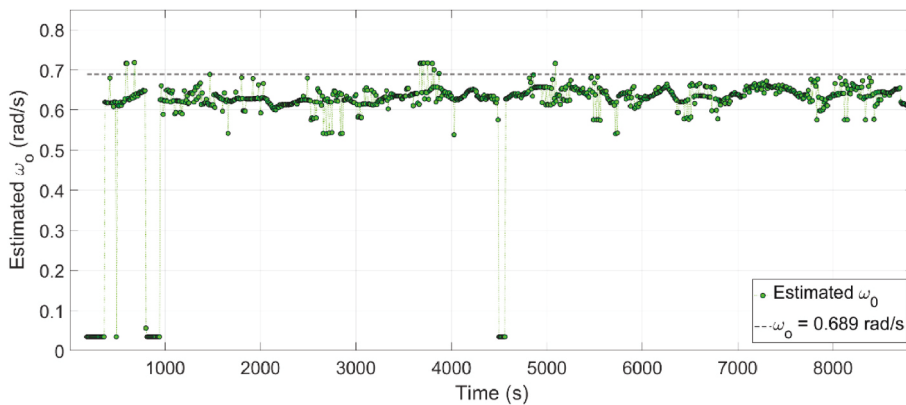

Fig. 8. Roll motion – Series 5.

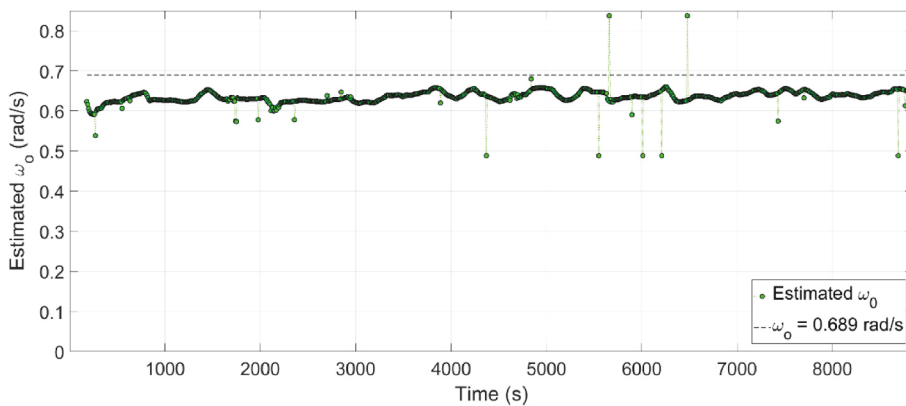**Fig. 9.** Roll natural frequency estimation – Series 5.

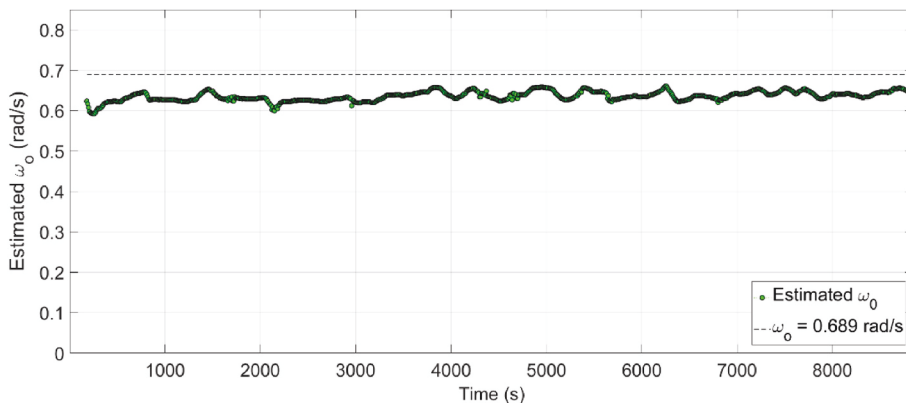**Fig. 10.** Roll natural frequency estimation with constraints – Series 5.

Fig. 11. Roll natural frequency estimation with constraints and Hampel filter – Series 5.

Table 5
Summary of results – Series 5.

	Methodology	Methodology with constraints	Methodology with constraints and Hampel filter
Median (rad/s)	0.633	0.635	0.635
P5 (rad/s)	0.540	0.619	0.621
P95 (rad/s)	0.666	0.655	0.655

situations, the median is very close to the target value with a maximum deviation of −21.94% and being in most of the cases around −8%.

Finally, it has to be mentioned that during the entire campaign the wave height was not higher than 1 m and at anytime resonance did not take place. Due to this fact, the roll amplitude was quite low, below 5°. Furthermore, there were some changes in the angle of heel during navigation. Considering that the test vessel was working as a pair trawler, these changes could be motivated by the modification of the two trawling vessels heading that resulted in variations of the net tension that affected the angle of heel.

Table 6
Summary of results.

Time series	Target ω_0 (rad/s)	Methodology				Methodology with constraints				Methodology with constraints and Hampel filter			
		Median (rad/s)	P5 (rad/s)	P95 (rad/s)	Deviation to the target value (%)	Median (rad/s)	P5 (rad/s)	P95 (rad/s)	Deviation to the target value (%)	Median (rad/s)	P5 (rad/s)	P95 (rad/s)	Deviation to the target value (%)
1	0.691	0.035	0.035	0.628	−94.93	0.599	0.489	0.645	−13.31	0.600	0.489	0.643	−13.16
3	0.691	0.082	0.035	0.617	−88.13	0.602	0.526	0.627	−12.88	0.603	0.539	0.627	−12.74
5	0.689	0.633	0.540	0.666	−8.13	0.635	0.619	0.655	−7.84	0.635	0.621	0.655	−7.84
8	0.689	0.648	0.594	0.685	−5.95	0.642	0.626	0.666	−6.82	0.643	0.628	0.665	−6.68
9	0.689	0.644	0.577	0.676	−6.53	0.641	0.624	0.668	−6.97	0.641	0.630	0.667	−6.97
11	0.689	0.636	0.540	0.706	−7.69	0.634	0.575	0.670	−7.98	0.634	0.575	0.668	−7.98
12	0.689	0.629	0.526	0.669	−8.71	0.634	0.613	0.659	−7.98	0.634	0.614	0.659	−7.98
13	0.689	0.595	0.035	0.647	−13.64	0.612	0.561	0.645	−11.18	0.613	0.563	0.645	−11.03
14	0.664	0.562	0.035	0.606	−15.84	0.568	0.489	0.599	−14.46	0.569	0.489	0.600	−14.30
15	0.702	0.548	0.035	0.612	−21.94	0.546	0.489	0.582	−22.22	0.548	0.489	0.583	−21.94
16	0.701	0.475	0.035	0.582	−32.24	0.551	0.489	0.608	−21.51	0.553	0.489	0.609	−21.23

Table 7
Summary of obtained *GM* and its deviation.

Time series	Target *GM* (m)	Methodology		Methodology with constraints		Methodology with constraints and Hampel filter	
		Obtained *GM* (m)	Deviation to the target value (%)	Obtained *GM* (m)	Deviation to the target value (%)	Obtained *GM* (m)	Deviation to the target value (%)
1	0.498	0.001	−99,743%	0,375	−24.794%	0.376	−24.542%
3	0.498	0.007	−98.591%	0.378	−24.038%	0.380	−23.786%
5	0.496	0.418	−15.675%	0.421	−15.141%	0.421	−15.141%
8	0.496	0.438	−11.631%	0.430	−13.260%	0.432	−12.990%
9	0.496	0.433	−12.719%	0.429	−13.530%	0.429	−13.530%
11	0.496	0.422	−14.874%	0.420	−15.408%	0.420	−15.408%
12	0.496	0.413	−16.737%	0.420	−15.408%	0.420	−15.408%
13	0.496	0.370	−25.495%	0.391	−21.177%	0.392	−20.919%
14	0.460	0.330	−28.329%	0.337	−26.790%	0.338	−26.532%
15	0.514	0.313	−39.014%	0.311	−39.459%	0.313	−39.014%
16	0.513	0.236	−54.091%	0.317	−38.224%	0.319	−37.775%

6. Conclusions

In this work, the performance of a methodology for estimating the vessel's roll natural frequency in real-time, and based on the spectral analysis of roll motion, has been tested in a real environment. Furthermore, some improvements to this methodology have been presented.

The sea trials consisted of a daily fishing campaign of a medium-sized pair stern trawler in Galician waters. During the trials ship motions, route, speed, loading condition and sea state have been monitored.

The analysis of the obtained data has demonstrated that the performance of the proposed methodology is satisfactory and it has been improved with the addition of the constraints and the Hampel filter.

To conclude, despite the fact that the methodology has been tested in a real environment, more sea trials would be needed to validate it in different and more severe sea states.

CRediT authorship contribution statement

Lucía Santiago Caamaño: Conceptualization, Methodology, Software, Validation, Formal analysis, Investigation, Writing – original draft, Writing – review & editing, Visualization. **Marcos Míguez González:** Conceptualization, Methodology, Software, Investigation, Resources, Writing – original draft, Writing – review & editing, Visualization, Supervision, Project administration, Funding acquisition. **Sandra Allegue García:** Methodology, Software, Validation, Formal analysis, Visualization. **Vicente Díaz Casás:** Conceptualization, Resources, Supervision, Project administration, Funding acquisition.

Declaration of competing interest

The authors declare that they have no known competing financial interests or personal relationships that could have appeared to influence the work reported in this paper.

References

Gudmundsson, A., 2013. The FAO/ILO/IMO safety recommendations for decked fishing vessels of less than 12 metres in length and undecked fishing vessels – a major milestone to improve safety for small fishing vessels. In: Proceedings of the 13th International Ship Stability Workshop, pp. 1–9. Brest.

IMO, 2008. International Code on Intact Stability (2008 IS Code). International Maritime Organization (IMO), London, UK.

Jensen, O.C.C., Petursdottir, G., Holmen, I.M., Abrahamsen, A., Lincoln, J., 2014. A review of fatal accident incidence rate trends in fishing. Int. Marit. Health 65, 47–52. https://doi.org/10.5603/IMH.2014.0011.

Koyama, T., 1982. On a micro-computer based capsize alarm system. In: Proceedings of the 2nd International Conference of Stability of Ship and Ocean Vehicles. Tokyo, Japan.

Míguez González, M., Bulian, G., 2018. Influence of ship dynamics modelling on the prediction of fishing vessels roll response in beam and longitudinal waves. Ocean Eng. 148, 312–330. https://doi.org/10.1016/j.oceaneng.2017.11.032.

Míguez González, M., Bulian, G., Santiago Caamaño, L., Díaz Casás, V., 2017. Towards real-time identification of initial stability from ship roll motion analysis. In: Proceedings of the 16th International Ship Stability Workshop. Belgrade, Serbia.

Míguez González, M., Díaz Casás, V., Santiago Caamaño, L., 2016. Real-time stability assessment in mid-sized fishing vessels. In: Proceedings of the 15th International Ship Stability Workshop, pp. 201–208.

Míguez González, M., Santiago Caamaño, L., Díaz Casás, V., 2018. On the applicability of real time stability monitoring for increasing the safety of fishing vessels. In: Proceedings of the 13th International Conference on the Stability of Ships and Ocean Vehicles. Kobe, Japan.

Míguez González, M., Sobrino Caamaño, P., Tedín Álvarez, R., Díaz Casás, V., Martínez López, A., López Peña, F., 2012. Fishing vessel stability assessment system. Ocean Eng. 41, 67–78. https://doi.org/10.1016/j.oceaneng.2011.12.021.

Pearson, R.K., Neuvo, Y., Astola, J., Gabbouj, M., 2016. Generalized Hampel filters. EURASIP J. Appl. Signal Process. 87 https://doi.org/10.1186/s13634-016-0383-6, 2016.

Puertos del Estado, 2020. Oceanografía - Predicción de oleaje, nivel del mar: boyas y mareógrafos [WWW Document]. URL. http://www.puertos.es/es-es.

Santiago Caamaño, L., Galeazzi, R., Nielsen, U.D., Míguez González, M., Díaz Casás, V., 2019. Real-time detection of transverse stability changes in fishing vessels. Ocean Eng.

Santiago Caamaño, L., Míguez González, M., Díaz Casás, V., 2018. On the feasibility of a real time stability assessment for fishing vessels. Ocean Eng. 159, 76–87. https://doi.org/10.1016/j.oceaneng.2018.04.002.

Scarponi, M., 2017. Use of the Wolfson stability guidance for appraising the operational stability of small fishing vessels. In: Proceedings of the 16th International Ship Stability Workshop. Belgrade, Serbia.

Terada, D., Hashimoto, H., Matsuda, A., Umeda, N., 2018a. Direct estimation of natural roll frequency using onboard data based on a Bayesian modeling procedure. In: Proceedings of the 13th International Conference on the Stability of Ships and Ocean Vehicles. Kobe, Japan.

Terada, D., Tamashima, M., Nakao, I., Matsuda, A., 2018b. Estimation of metacentric height using onboard monitoring roll data based on time series analysis. J. Mar. Sci. Technol. https://doi.org/10.1007/s00773-018-0552-4.

Viggosson, G., 2009. The Icelandic information system on weather and sea state related to fishing vessels crews and stability. In: World Fishing Exhibition. Vigo, Spain.

Wolfson Unit, 2004. Research Project 530. Simplified Presentation of FV Stability Information - Phase 1. Final Report. University of Southampton.

Womack, J., 2003. Small commercial fishing vessel stability analysis: where are we now? Where are we going? Mar. Technol. 40, 296–302.